Article Type: ***Methods*** contribution to ***Ecology Letters***

Title: TRAMPOline: a Temporal Relative Abundance-focused Multi-sPecies Occupancy model, illustrated using a fossil community

Running head: Relative abundance occupancy model

Authors:

Trond Reitan (trond.reitan@ibv.uio.no, Natural History Museum, University of Oslo, Norway)

Torbjørn Ergon (t.h.ergon@ibv.uio.no, Centre for Ecological and Evolutionary Synthesis, Department of Biosciences, University of Oslo, Norway)

Lee Hsiang Liow* (l.h.liow@nhm.uio.no, Natural History Museum, University of Oslo, Norway)

* corresponding author

Key words: occupancy models, relative abundance, Bayesian, sites, sub-samples, fossil record, sessile communities

Statement of authorship: LHL conceived the project, performed the field and lab work. LHL and THE developed earlier versions of the model. TR brought the model development to completion, wrote the code and performed the analyses. TR and LHL wrote the first draft of the paper and all authors contributed substantially to revisions.

Data accessibility statement: Should this manuscript be accepted, the data supporting the results will be archived in an appropriate public repository and the data DOI will be included at the end of the article. Code and data for review are available at https://github.com/trondreitan/TRAMPOline

Word count in main text = 4776; **No. references** = 29; **No. figures** = 6

Abstract

The relative abundance of species is temporally varying, but estimating abundance, given incomplete and biased sampling is challenging. Here, we describe a new occupancy model, TRAMPOline (Temporal Relative Abundance-focused Multi-sPecies Occupancy model) in a hierarchical Bayesian framework, where occupancy and detection are modeled as a means to estimate relative abundance. TRAMPOline can be applied to temporal occupancy data with sub-samples. We demonstrate TRAMPOline using a fossil community of benthic organisms to estimate relative abundance dynamics of several focal species over 2.3 million years, by drawing on information provided by non-focal species observed in the same community. We expanded TRAMPOline by adding random effects of species and time-intervals (geological formations) and explored potential explanatory factors (paleoenvironmental proxies) and temporal autocorrelation that could provide extra information on unsampled geological time-intervals. TRAMPOline is applicable across a wide range of questions on species-level dynamics in contemporary and palaeoecological community settings.

Introduction

Occupancy modeling in statistical ecology (King 2014) seeks to tease apart true site-occupancy and observations of species within sites by the explicit modeling of both ecological and detection processes (MacKenzie *et al.* 2017). Occupancy data are commonly collected as presence-absence data replicated within multiple sites. While occupancy probability is often the focus of occupancy modeling, it is also used to monitor the persistence of populations, estimate species richness, understand habitat preferences and to infer abundance (MacKenzie *et al.* 2017), the last of which is the our focus here.

Understanding the complex drivers of population dynamics and their interactions require robust empirical estimates of changing abundance (Sutherland *et al.* 2013), Here we develop TRAMPOline, a Temporal Relative Abundance-focused Multi-sPecies Occupancy model that can be applied to communities where data are organized as sites in which sub-sites are observed for multiple species over multiple time-intervals. We will demonstrate our model with a fossil benthic community (see methods and SI) but our model is applicable to diverse systems and ecological disciplines, including contemporary sessile plant or marine benthic communities (Marine and Plant Ecology), other fossil data including pollen and microfossil communities (Archeology, Micropaleontology, Quaternary Science), as well as eDNA data (metagenomics) in which subsamples from sites are analysed separately, over several time-intervals.

In TRAMPOline, local abundance (i.e. site-level abundance, given occupancy), is derived from detection through a point-process assumption. Here, the detection of a species in a sub-sample within a site is derived from a Poisson process with expected value proportional to local abundance. Through this, our aim is to estimate relative abundance of multiple species while drawing on information from other species within the same community and integrating information from multiple sites across time. In contrast, early

63 occupancy models were applied to single-species and did not include counts within sites
64 (MacKenzie *et al.* 2002, 2003). Later, extra information harbored in data in the form of
65 multiple-encounters within sites, were embraced by occupancy modelers. The first model that
66 estimates abundance from occupancy data, including counts, for a single species, the Royle-
67 Nichols (RN) model, assumed that detection probability increases with local abundance
68 (Royle *et al.* 2005). Yamaura *et al.* (2010) then developed a model that combines the RN
69 model with a multi-species approach (Dorazio *et al.* 2006), in order to infer the number of
70 species in the community using data augmentation and by assuming that abundance affects
71 detection. The model we develop here is different from previous hierarchical multispecies
72 occupancy and abundance models (Iknayan *et al.* 2014; Devarajan *et al.* 2020) as these
73 models are focused on estimating species richness (including those that are undetected), but
74 leverage abundance for species richness estimation. Here we are conversely interested in
75 abundance. We factorize sampling (i.e. detection) into shared (species-independent) and
76 species-dependent components using random factors, such that the uncertainty for a given
77 time-interval is informed by the variation found in others. These random effects handle time-
78 interval specific sampling differences, as well as fluctuations common to all species involved,
79 i.e. components irrelevant to relative abundance.

80 By describing how the relative abundance, and secondarily, the occupancy probability
81 of various species have changed over time, TRAMPOline allows us to hypothesize the roles
82 of potential drivers of ecological waxing and waning. In this methodological contribution, we
83 briefly describe a empirical system to which TRAMPoline can be applied as an example, then
84 develop a model to extract relevant (paleo)ecological parameters from this system. Using
85 simulated data, we explore if ecological dynamics can be accurately inferred using our
86 model. Last, we discuss the utility of our model for diverse systems and suggest venues for
87 the expansion of our model.

Materials and methods

Study system

To illustrate how TRAMPOline can be applied, we use an empirical system of fossilized benthic organisms spanning 2.3 million years found in the Wanganui Basin, (Carter & Naish 1998; Proust *et al.* 2005; Pillans 2017) as detailed in the SI. We sampled 9 time-intervals in a total of 119 sites (see Fig. 1 for a schematic representation), in which the number of sub-samples varied between 30-50 (see Table S1 and SI for details). We tabulated the observed presence of three focal species namely *Antharcthoa tongima*, *Escharoides excavata* and *Arachnopusia unicornis* (Fig. S1) in each subsample for all 9 time-intervals and 119 sites. We also introduce a fourth "species", the superspecies, which represents all other bryozoan species excluding the three focal species. This superspecies information contributes to our estimates of relative abundance for the three focal species (see model description). Since the formations (time-intervals) were chosen because they are known to harbor bryozoans, the superspecies is assumed to always be present, i.e. occupancy probability=1. In other applications, the occupancy probability of the superspecies can be estimated within the model. Note that there is ample among-formation, within-formation and among-species variation in the ratio of examined shells with observations of encrusting bryozoans, where non-observation includes both the lack of detection and non- occupancy (Fig. S2).

Model description

Our main objective is to estimate the temporal (i.e. formation-to-formation) dynamics of relative abundances for each focal species using presence/absence observations on sub-samples (shells) from different sites (Fig.1, Fig. S1). There are two probabilities at play; the probability that a species occupied a given site i.e. the occupancy probability, Ψ, and the probability that a sub-sample has at least one observation of the focal species, given

occupancy, i.e., the detection probability, p. The probability that a species is found on a given sub-sample is thus Ψp, where Ψ operates on the site-level while p operates on the sub-sample-level. The occupancy and detection probabilities will be functions of various parameters and random factors, and can be specific to the site i belonging to a specific time-interval, and the species, s. Thus, we will write $\Psi_{i,s}(\theta)$ and $p_{i,s}(\theta)$ for the occupancy and detection probabilities respectively, where θ is the set of top parameters and random variables of the model in question (Fig. 2). The relative abundances for the focal species and time-intervals will be derived from these two sets of probabilities as such: the site-dependent detection probability is decomposed into a time-interval-dependent component and a local fluctuation. Working on the time-interval-dependent scale, a Poisson process with intensity proportional to the local abundance, given occupancy, determines the detection probability. The abundance of a species in a given time-interval is then the expected local abundance (unconditioned on occupancy), or in other words, local abundance given occupancy times the occupancy probability. This is determined up to an unknown proportionality constant, but where the latter drops out when calculating relative abundance.

We build our models in a step-wise fashion, starting with a standard occupancy model because it is the most familiar, then gradually adding complexity until we have a model with enough elements to allow for relative abundance estimates. The reason for this step-wise presentation is three-fold. The first is to put focus on each of the model components. Second, because MCMC convergence was possible to achieve only when we used the parameter estimates from a simpler model as the starting points for the next, more complex model. Thirdly, because we wanted to justify the model complexities we added, using the Bayes factor as measure of evidence (Jeffreys 1998).

1. The basic occupancy model

The simplest occupancy model (MacKenzie *et al.* 2002) contains only occupancy and detection probabilities such that number of sub-samples at site i with observations of species s is a zero-inflated binomial random variable.

$$y_{i,s} \sim zbin\left(N_i, p_{i,s}(\theta) = \text{logit}^{-1}(\beta_s), \Psi_{i,s}(\theta) = I(s = S) + I(s < S)\text{logit}^{-1}(\alpha_s)\right) \quad (1)$$

Here, N_i is the total number of sub-samples examined at site *i*. *I()* stands for the indicator function, which takes value 1 when the statement inside is true and 0 if it is false. The unconditional probability of detection is $p_{i,s}(\theta)\Psi_{i,s}(\theta)$. We express both occupancy and detection probabilities using a logit-transform, i. e. $\text{logit}(r) \equiv \log\left(\frac{r}{1-r}\right)$, where r is a probability, for the convenience of expanding the model in the next sections. The two parameters, α_s and β_s, (see Fig. 2) give regional (i.e. within the Wanganui Basin in our application) occupancy and detection probabilities for each species respectively, regardless of time-interval (formation). The parameter set is $\theta = \{\alpha_1, \cdots, \alpha_{S-1}, \beta_1, \cdots, \beta_S\}$, where *S* is the number of species (focus species plus superspecies). Even though we are currently describing a time-intervals-independent model, we write $\Psi_{i,s}(\theta)$ and $p_{i,s}(\theta)$, since occupancy and sampling will be derived from parameters that are both species-dependent and site-dependent (or in practice, time-interval dependent) later. Note however, that $\alpha_{s=S}$ does not appear in the model, as we assume that the superspecies is always present (leaving us with $2 \times S - 1$ parameters).

2. Including site-dependent random factors through overdispersion

Fluctuations in the local abundance of a species can be modelled by a per site, per species random factor. Here, site-dependent detection probability is allowed to vary around the median regional detection probability. If this random factor was normal on the logit-scale,

one could either estimate the random factors in a hierarchical Bayesian model or integrate over the logit-normal distribution, yielding an over-dispersed version of the binomial distribution (e.g. Harrison 2014). The latter option gives the logit-normal binomial distribution and simplifies the model, as it removes explicit site-dependency. This distribution does not, however, have a closed analytical expression (e.g. Schmettow 2009). If the random effects are instead beta-distributed, we can use the zero-inflated beta-binomial distribution, which does have an analytical expression.

$$y_{i,s} \sim z\beta bin\left(N_i, p_{i,s}(\theta) = \text{logit}^{-1}(\beta_s), \kappa_s, \Psi_{i,s}(\theta) = I(s = S) + I(s < S)\text{logit}^{-1}(\alpha_s)\right) \quad (2)$$

Here, κ_s describes the species-dependent overdispersion. The parameters set is now $\theta = \{\alpha_1, \cdots, \alpha_{S-1}, \beta_1, \cdots, \beta_S, \kappa_1, \cdots, \kappa_S\}$. The detection and occupancy probabilities depend on the identity of the time-interval that site belongs to, rather than the site itself, as the overdisperson account for the variation among sites (at this point no time-interval dependency has been added). This also holds for later models presented here. The probability of y observations out of n sub-samples from the zero-inflated beta-binomial distribution with detection probability, p, overdispersion parameter, κ, and zero-inflation, Ψ, is defined as:

$$P_{z\beta bin}(y|n, p, \kappa, \Psi) = (1\text{-}\Psi)I(y = 0) + \Psi\frac{\Gamma(n+1)\Gamma\left(y+\frac{p}{\kappa}\right)\Gamma\left(n-y+\frac{1-p}{\kappa}\right)\Gamma\left(\frac{1}{\kappa}\right)}{\Gamma(y+1)\Gamma(n-y+1)\Gamma\left(n+\frac{1}{\kappa}\right)\Gamma\left(\frac{p}{\kappa}\right)\Gamma\left(\frac{1-p}{\kappa}\right)} \quad (3)$$

The first term of the right hand-side of Eqn (3) up to (but not including) the fractional expression, describes the zero-inflation, while the second, fractional part describes the beta-binomial distribution.

3. Including species- and formation-dependent random factors

We now introduce temporal dynamics by using time-interval-dependent random factors (e.g. Pacifici *et al.* 2016) that are species-independent, i.e. they summarize dynamics common to all species in the community. For the detection probability, the random effects imply fluctuations in the sampling as well as in average density of the community of species in question. For occupancy, the random effects allow fluctuations in the overall presence of species in question. The time-intervals with richer data can thus inform estimates for those with sparser data. The model is now:

$$y_{i,s} \sim z\beta bin\left(N_i, p_{i,s}(\theta) = \text{logit}^{-1}\left(\beta_s + u_{f(i)}\right), \kappa_s, \Psi_{i,s}(\theta) = I(s = S) + I(s < S)\text{logit}^{-1}\left(\alpha_s + v_{f(i)}\right)\right) \quad (4a)$$

$$u_f \sim N(0, \sigma_u^2),\ v_f \sim N(0, \sigma_v^2), \quad (4b)$$

where $f(i)$ is the time-interval that site i belongs to, u_f and v_f are the new time-interval-dependent random effects and σ_v and σ_u are the standard deviations of these effects, for detection and occupancy, respectively. Now, $\theta = \{\alpha_1, \cdots, \alpha_{S-1}, \beta_1, \cdots, \beta_S, \kappa_1, \cdots, \kappa_S, \sigma_u, \sigma_v, u_1, \cdots, u_F, v_1, \cdots, u_F\}$, where F is the number of time-intervals (geological formations in our empirical example).

While this model (Eqn 4) does allow for dynamics due to time variations in the whole set of species in the region, the probabilities vary in sync for the different species. In order to facilitate dynamics that permit fluctuations in the relative species-dependent abundances, we need random effects that depend on species and formation combinations. When doing so, we have:

$$y_{i,s} \sim z\beta bin\left(N_i, p_{i,s}(\theta) = \text{logit}^{-1}\left(\beta_s + u_{f(i)} + \varepsilon_{f(i),s}\right), \kappa_s, \Psi_{i,s}(\theta) = I(s = S) + I(s < S)\text{logit}^{-1}\left(\alpha_s + v_{f(i)} + \delta_{f(i),s}\right)\right) \quad (5a)$$

$$u_f \sim N(0, \sigma_u^2),\ v_f \sim N(0, s\sigma_v^2),\ \delta_{f,s} \sim N\left(0, \sigma_{\delta,s}^2\right),\ \varepsilon_{f,s} \sim N\left(0, \sigma_{\varepsilon,s}^2\right) \quad (5b)$$

where $\varepsilon_{f,s}$ and $\delta_{f,s}$ are the new time-interval- and species-dependent random effects and $\sigma_{\varepsilon,s}$ and $\sigma_{\delta,s}$ are the standard deviations of these effects, for detection and occupancy, respectively. Our inferred abundances are averages over time as well as space, so it can is better described as being proportional to an temporally-averaged density and is hence continuous rather than integer-valued.

The time-interval dependent random effects (u_f and v_f) introduced in Eqn. (4) do not affect the estimation of relative overall abundances (since these are estimated for each formation), but will take away pure formation dependencies from the species- plus time-interval dependent random variables, thus removing possible source of bias and make our uncertainty estimates more precise.

The parameter set is now $\theta = \{\alpha_1, \cdots, \alpha_{S-1}, \beta_1, \cdots, \beta_S, \kappa_1, \cdots, \kappa_S, \sigma_u, \sigma_v, \sigma_{\delta,1}, \cdots, \sigma_{\delta,S-1}, \sigma_{\varepsilon,1}, \cdots, \sigma_{\varepsilon,S}, u_1, \cdots, u_F, v_1, \cdots, u_F, \delta_{1,1}, \cdots, \delta_{F,S}, \varepsilon_{f,s}, \cdots, \varepsilon_{F,S}\}$. Specifically, our top parameters (as opposed to the random factors) are $\{\alpha_1, \cdots, \alpha_{S-1}, \beta_1, \cdots, \beta_S, \kappa_1, \cdots, \kappa_S, \sigma_u, \sigma_v, \sigma_{\delta,1}, \cdots, \sigma_{\delta,S-1}, \sigma_{\varepsilon,1}, \cdots, \sigma_{\varepsilon,S}\}$. We log-transformed all positive-valued parameters including the standard deviations and over-dispersion parameters, so that the re-parametrized parameter set allows values along the entire real line. With 3 species and one super-species (S=4), our application has *20* (*5*×*S*) top-parameters. In addition, the inference also needs to handle 81 ((*2S+1*)×*F*) random variables (Eqn 5b). We call Eqn (5) the "full model" i.e. TRAMPOline, since it has all the necessary component for estimating the dynamics of relative abundance (shown in Fig. 2).

4. A step-wise approach for improving estimation

Because the full model is fairly complex and required hierarchically arranged random effects, we utilized Markov chain Monte Carlo (MCMC) sampling for inference (SI section "MCMC for statistical inference"). We used common estimated parameter values from a simpler model when starting a more complex model, in a step-wise fashion (i.e. from Eqn 1 to 2 to …5) as preliminary analyses often failed when starting from a random place in the parameter space. In doing so, we also tested if each increasingly complex model explained the data better, using Bayes factors.

5. Incorporating explanatory variables

We expanded our full model (Eqn 5) by including temporal explanatory variables – in our empirical example pertaining to paleoclimate, as well as auto-correlated processes by using an Ornstein–Uhlenbeck process (SI sections "Model expansions that include explanatory variables" and "Introducing correlations in the random effects") although results from these are not detailed in the main text. Our motivation for examining and testing these expansions was to develop extended models that predict relative abundances in unmeasured time-intervals with more precision than just using the time-interval-independent median values derived from α_s and β_s. We impose a quadratic term for our explanatory variables (on detection probability, occupancy probability or both) as each species should thrive at an (different) optimal climate, with a given tolerance width. For demonstration, we use two related but different paleoclimate proxies, namely the global $\partial^{18}O$ data (data from Lisiecki & Raymo 2005) and the North Atlantic magnesium/calcium (Mg/Ca) ratios (data from Sosdian & Rosenthal 2009), both based on measurements from benthic foraminiera, as explanatory variables. These contain complex signals of sea temperature, ice-volume and sea-level changes, all of which potentially affect both the population growth rates (through optimal

260 temperatures and the availability of substrate species) and detection probabilities (through
261 sea-level changes) of our focal species. Whether other applications of TRAMPOline will
262 benefit from such model extensions is naturally context-dependent..
263
264 6. Estimating relative abundances
265 In this section we estimate the relative abundance estimates of a given species in a given
266 formation. The relative abundance of a species is proportional to the sum of its local
267 abundances given occupancy, $\lambda_{i,s}$, times its occupancy probability $\Psi_{i,s}$. For the ease of
268 reading, we suppress denoting that the elements described are all functions of the model
269 parameter set in this section. Since our model does not contain any site-dependent
270 components (except that absorbed by overdispersion), relative abundance estimate $A_{f,s}$ can be
271 expressed using formation (time-interval) indexes (*f*) instead of site indexes (*i*) as such:
272
273 $$A_{f,s} \propto \Psi_{f,s}\lambda_{f,s}. \quad (6)$$
274
275 However, the detection probability, $p_{f,s}$, and the local abundance, $\lambda_{f,s}$, do not scale
276 proportionally to each other. This is because while detection probability has an upper limit,
277 local abundance (i.e. counts of individuals of a given species in a defined area at a given
278 time) does not. To obtain relative abundances, a link between the inferred detection
279 probability of a species in a given formation, $p_{f,s}$, and the time-averaged abundance, $\lambda_{f,s}$,
280 must be formulated. Here we assume that the number of individuals of a species in each sub-
281 sample can be described by a Poisson process, where the Poisson parameter is proportional to
282 the time-averaged abundance. Thus
283

$$P(\text{at least one individual of species } s \text{ is found in the sub} - \text{sample in an occupied site in time} - \text{interval } f) = p_{f,s} = 1 - e^{-k\lambda_{f,s}} \quad (7)$$

where k is the proportionality constant. In our application, k will be affected by the preservation probability of bryozoans in the formation, which will in turn affect the time-interval-dependent random effects in Eqns (4-5). In other systems, "preservation" is simply a common observational filter that may or may not be necessary. If such a filter is unnecessary, the time-interval dependent and random effects may be excluded. The time-interval-dependent random effects and k, are also affected by species-independent fluctuations in the regional overall abundance. We assume that k is species-independent (i.e. we assume that individuals, regardless of their species identity, in a given time-interval have equal chances of getting preserved). Eqn (7) ensures that while the temporally-averaged abundance of species s can be any positive real number larger than zero, the detection probability will be between zero and one. Up to the proportionality constant, k, Eqn (7) is Eqn (1) in (Yamaura *et al.* 2010). In most, if not all previous occupancy models that incorporate counts, spatial area is strictly defined and the time window of sampling so short that one can assume the counts of individuals (integers) inhabiting that area do not vary over the given study. In contrast, the abundances we are interested in are averaged over both time and space such that they must be represented by positive real numbers rather than integers. We now calculate the relative abundance, $\mathrm{R}_{f,s}$ using Eqs. (6) and (7):

$$\mathrm{R}_{f,s} = \frac{A_{f,s}}{\sum_{s'=1}^{S} A_{f,s'}} = \frac{\Psi_{f,s}\lambda_{f,s}}{\sum_{s'=1}^{S} \Psi_{f,s'}\lambda_{f,s'}} = \frac{k\Psi_{f,s}\lambda_{f,s}}{\sum_{s'=1}^{S} k\Psi_{f,s'}\lambda_{f,s'}} = \frac{\Psi_{f,s}\log(1-p_{f,s})}{\sum_{s'=1}^{S} \Psi_{f,s'}\log(1-p_{f,s'})} \quad (8)$$

Note that the proportionality constant in Eqn. 7 cancels out. Thus, the relative abundance of a focal species can be estimated from the components of the occupancy model.

For an alternative modelling approach to estimate relative abundance, built-up from the local abundance-related parameters, $\lambda_{f,s}$, rather than detection probabilities, see SI "Description of the local abundance focused model".

7. Simulations

We performed two sets of simulations. The first "parameter-focused simulation study" was performed to check how well estimated parameters and derived quantities (occupancy probabilities, detection probabilities and relative abundances) can be inferred from data. The second "occupancy dynamics-focused simulation study" was performed to check under what sampling regimes we could detect occupancy probability dynamics when the parameters were as estimated in the empirical data.

For the parameter-focused simulation study, we generated 100 datasets from a common parameter set that reflects idealized but plausible scenarios for the four species, and analyzed each dataset separately. All simulations used 10 sites per formation, closer to the lower end of our empirical data (Table S1) and 60 shells per site, closer to the maximum of our empirical data, the upper limit of what is reasonable in the field. We varied the species-dependent constants for occupancy and detection among the species. For instance, species 3 (SI Figs. S16, S17) is assigned an elevated detection but lower occupancy probabilities compared to estimates from our actual dataset. This would decrease estimation uncertainty compared to our actual data, thus making bias easier to detect and occupancy easier to untangle from detection. Species 1 was assigned occupancy dynamics (SI Fig. S16) and species 2 was assigned detection dynamics (SI Fig. S17). While it might have been ideal to

simulate all combinations of parameters, it is not computationally realistic. We urge future users of TRAMPOline to run simulations to verify estimates specific to their needs, such as we have done here. See SI section "Parameter-focused simulation study" for further details.

For the occupancy dynamics-focused simulation study, we generated data under different sampling intensisites (10, 20, 30, 50, 100 and 1000 sites per formation and 60, 100, 200, 400 and 1000 shells per site) and analyzed these data using the model and parameter estimates developed for our empirical data data. Here, we were specifically interested in checking whether occupancy dynamics are detectable under different sampling scenarios (see SI "Occupancy dynamics-focused simulation study").

Results

Empirical findings

We found that including both the time-interval-dependent (i.e. formation-dependent) random effects (introduced in Eqn 4) and the time-interval- and species-dependent random effects (introduced in Eqn 5) improved the description of our empirical data (SI Table S2). In other words, the full model described in Eqn (5) (Fig. 2) was preferred based on Bayes Factors, implying that the occupancy and detectability of the different bryozoan species varied with time-intervals (formation). However, including paleoclimate explanatory variables or auto-correlated random effects did not improve our model (SI Table S2). In other words, we currently do not have any component in our models that allow us to predict relative abundance for unmeasured time-intervals using information beyond the median detection and occupancy probabilities given by α_s and β_s for our empirical data. The Bayes factor did not resolve the choice between the "local abundance focused model" and the full model, and it gave highly similar estimates of relative abundances (see SI).

The overdispersion parameters, κ_s,were estimated to 0.09, 0.05, 0.04 and 0.07 for *Antharcthoa tongima*, *Escharoides excavata* and *Arachnopusia unicornis* and the superspecies, respectively (see Table S3 for credibility bands), where $\kappa_s = 0$ means no overdispersion. While these estimates are very close to zero, they represent overdispersion that effectively double the variance, compared to no overdispersion (see SI Fig. S6).

The uncertainty surrounding the occupancy probability of each of the focal species is quite large (Fig. 3), where we cannot establish that occupancy is well below 1.0 for any combination of species and formation. Detection probabilities estimated from our full model are also shown in Fig. 4. Note that the relative changes in detection probabilities are similar to the dynamics of the raw data (Fig. S2).

By combining occupancy and detection probabilities, we can estimate the relative abundance using Eqn (8) (Fig. 5 and SI Figs. S5 and S11). The relative abundances of the superspecies and *A. tongima* are estimated with relatively high precision and vary significantly over time. The relative abundances of *E. excavata* and *A. unicornis* are estimated with much greater uncertainty.

Simulation results

The parameter-focused simulation study shows a spread of the estimates around the true values for both parameters (SI Figs. S12-15) and the derived quantities of occupancy probabilities (SI Fig. S16), detection probabilities (SI Fig. S17) and relative abundances (Fig. 6). Although these estimates are spread quite evenly around both sides of the actual values, minute biases, expected given our informative priors and non-linear transformations, were found, but not cause for worry (see the SI section on the parameter-focuses simulation study).

The results of occupancy dynamics-focused simulation study that is specific to our empirical study indicate that even large volumes of data cannot distinguish occupancy

dynamics (Table S4) within or among the focal species with the possible exception of *Escharoides excavata* (see SI for details).

Discussion

Ecologists are interested in estimating changing relative abundance because it is a prime window into population dynamics (Sutherland *et al.* 2013). On a shorter time scale, understanding how environmental attributes and species traits affect population changes within communities are not only key to ecological understanding but also conservation management (Bowler *et al.* 2018). On a longer time scale, the changing the relative abundance of fossil taxa have, in addition, the potential for supplying direct information on the evolution of phenotypes and changing ecological interactions (e.g. Liow *et al.* 2019) to enable linking paleoecological dynamics to evolutionary changes. However, estimating abundance or density in nature is challenging, regardless of the characteristics of organism (e.g. sessile or motile, small-bodied or large-bodied), the type of data (e.g. direct counts, capture-recapture data), or the time-scale involved (e.g. seasonal, yearly or paleoecological data). Occupancy modeling, which explicitly models sampling probabilities when estimating parameters of biological interest, including changes in relative abundance, is one powerful way of incorporating different sources of data heterogeneity and uncertainty. While occupancy modeling is increasingly widespread in "traditional" ecological studies (Bailey et al. 2013), is yet to be applied regularly in eDNA or metagenomics surveys (Da Silva Neto *et al.* 2020; McClenaghan *et al.* 2020) and also lags behind in paleoecology (Liow 2013). We believe TRAMPOline has broad applicability in many systems where sub-samples within sites are surveyed with relative ease and where relative abundance rather than species richness is of interest.

406 To briefly elaborate on the applicability of TRAMPOline in paleoecological settings,
407 we emphasize that fossil sampling probability is far from one, not least because preservation
408 is far from guaranteed (Kidwell & Holland 2002). Traditionally in paleoecology, however,
409 there is an underlying assumption, usually implicit, that preservation (and hence the sampling
410 of preserved organisms) is comparable across samples and sites, sometimes even across time-
411 intervals, as long as sampling is standardized. Here, what we termed "detection ratios" are
412 usually presented as estimates of relative abundance (Kidwell 2002; Currano *et al.* 2008;
413 Espinosa *et al.* 2020) . However, we know from simulations and ecological studies that this
414 assumption is problematic (Iknayan *et al.* 2014; MacKenzie *et al.* 2017). Not only is it
415 important to progress beyond tabulations of paleoecological data for improved inferences,
416 parameters estimated using fossil data should be as comparable as possible with the those
417 estimated using living organisms. This will allow us to infer historical baselines for
418 conservation applications and to gain a better understanding of changing biota over longer
419 timescales for which we may have analogue crisis situations (Harnik *et al.* 2012).
420 Instead of using the observed presence or absence of species, we could have instead
421 used the counts of the number of individuals of a given species in each sub-sample. If we
422 used the latter, we would have built a model similar to an N-mixture model (Royle 2004).
423 However, the sub-samples in our example (shells or fragments thereof) varied in volume and
424 these differences are expected to affect the number of individuals (colonies in our case). But
425 shell size (i.e. sub-sample size) was not quantified, hence a random factor for sub-samples
426 would be needed to account for this variation. This inclusion, however, would massively
427 increase model complexity while introducing an uncertainty that would make the extra
428 information (counts per shell in our case) of little relevance. Since the computational cost
429 would dramatically increase while the outcome was intuitively not expected to improve

significantly, we decided against this route for our empirical demonstration. However, in other applications, sub-sample size can be standardized or controlled for.

We note several extensions to our models that can be considered, with regards to our empirical system. First, there are other sources of variation that we did not take into account, including the species of the shell substrate (e.g. some were cockles and others were scallops) and their size as mentioned above, both of which may be selected by the bryozoan species involved and/or preferentially preserved. The information can be potentially collected in future studies that could improve the estimates. Second, we could potentially handle the number of colonies observed for each focal species per shell, since this could give an extra indication of the local abundance of each species. However, in addition to more time-consuming data collection, one would also have to introduce a random variable per shell, as mentioned above. Third, there are huge spans of time in which we are not able to sample bryozoans because suitable material was not deposited. We used two paleoenvironmental proxies (∂^{18}O and Mg/Ca ratios) as covariates in expanded models (SI) in hope that they contained predictive information we could use on unsampled time-intervals. While neither of the two we had published data for were informative, it is possible that other paleoevironmental proxies, published or yet to be collected, could be used for this purpose.

One lesson learnt from our empirical modelling is that while we are able to estimate the dynamics of relative abundance (Fig. 5), the dynamics of occupancy are challenging to grasp in our system. Our occupancy dynamics-focused simulations show that reliably getting occupancy estimates that vary from formation to formation requires unfeasibly intense sampling protocols for our choice of species, with the possible exception of *Escharoides excavata* though the requirements there were also quite demanding (see SI). The estimated occupancy probabilities are high while the detection probabilities are relatively low (Figs. 3 and 4), a reason why occupancy probabilities and hence dynamics were elusive. In retrospect,

455 if we had chosen species that were more selective of the sites they choose settle in, the
456 occupancy dynamics may have been easier to estimate. Detecting occupancy dynamics was
457 not the principal goal of the study, but in studies where this is of principal concern, such
458 issues should be considered before extensive data collection.
459
460 With our work, we hope that more paleoecologists will consider occupancy modeling
461 as a means to estimate relevant ecological parameters; ecological modelers will pick up
462 where we left off to improve the inference of biologically relevant parameters using a
463 challenging but rich fossil record; and that biologists with very different types of data but
464 similar data structure and questions, such as those analyzing site-specific eDNA to
465 understand relative abundance, will find use for TRAMPOline.
466
467 **Code**
468 The code and data for all analyses are provided at
469 https://github.com/trondreitan/TRAMPOline
470
471 **Acknowledgements**.
472 We thank P. D. Taylor, S. Rust, D. P. Gordon and K. L. Voje for field work and taxonomic
473 identifications and E. Di Martino for taxonomic identifications. This project has received
474 funding from the European Research Council (ERC) under the European Union's Horizon
475 2020 research and innovation programme (grant agreement No 724324 to LHL) and the
476 Norwegian Research Council Grant 235073/F20 (PI LHL).
477
478 **References**
479 Bowler, D.E., Heldbjerg, H., Fox, A.D., O'Hara, R.B. & Böhning-Gaese, K. (2018).
480 Disentangling the effects of multiple environmental drivers on population changes

within communities. *J. Anim. Ecol.*, 87, 1034–1045.

Carter, R.M. & Naish, T.R. (1998). A review of Wanganui Basin, New Zealand: global reference section for shallow marine, Plio-Pleistocene (2.5-0 Ma) cyclostratigraphy. *Sediment. Geol.*, 122, 37–52.

Currano, E.D., Wilf, P., Wing, S.L., Labandeira, C.C., Lovelock, E.C. & Royer, D.L. (2008). Sharply increased insect herbivory during the Paleocene-Eocene Thermal Maximum. *Proc. Natl. Acad. Sci.*, 105, 1960–1964.

Devarajan, K., Morelli, T.L. & Tenan, S. (2020). Multi-species occupancy models: review, roadmap, and recommendations. *Ecography (Cop.).*, 43, 1612–1624.

Dorazio, R.M., Royle, J.A., Soderstrom, B. & Glimskar, A. (2006). Estimating species richness and accumulation by modeling species occurrence and detectability. *Ecology*, 87, 842–854.

Espinosa, B.S., D'Apolito, C., Silva-Caminha, S.A.F., Ferreira, M.G. & Absy, M.L. (2020). Neogene paleoecology and biogeography of a Malvoid pollen in northwestern South America. *Rev. Palaeobot. Palynol.*, 273.

Harnik, P.G., Lotze, H.K., Anderson, S.C., Byrnes, J.E., Finkel, Z. V, Finnegan, S., *et al.* (2012). Extinctions in ancient and modern seas. *Trends Ecol. Evol.*, 27, 608–617.

Harrison, X.A. (2014). Using observation-level random effects to model overdispersion in count data in ecology and evolution. *PeerJ*, 2:e616.

Iknayan, K.J., Tingley, M.W., Furnas, B.J. & Beissinger, S.R. (2014). Detecting diversity: emerging methods to estimate species diversity. *Trends Ecol. Evol.*, 29, 97–106.

Jeffreys, H. (1998). *The Theory of Probability*. 3rd edn. Oxford University Pres.

Kidwell, S.M. (2002). Time-averaged molluscan death assemblages: Palimpsests of richness, snapshots of abundance. *Geology*, 30, 803–806.

Kidwell, S.M. & Holland, S.M. (2002). The quality of the fossil record: Implications for

506 evolutionary analyses. *Annu. Rev. Ecol. Syst.*, 33, 561–588.
507 King, R. (2014). Statistical Ecology. *Annu. Rev. Stat. Its Appl.*, 1, 401–426.
508 Liow, L.H., Reitan, T., Voje, K.L., Taylor, P.D. & Di Martino, E. (2019). Size, weapons, and
509 armor as predictors of competitive outcomes in fossil and contemporary marine
510 communities. *Ecol. Monogr.*, 89, e01354.
511 Lisiecki, L.E. & Raymo, M.E. (2005). A Pliocene-Pleistocene stack of 57 globally distributed
512 benthic δ18O records. *Paleoceanography*, 20, PA1003.
513 MacKenzie, D., Nichols, J., Royle, A., Pollock, K., Bailey, L. & Hines, J. (2017). *Occupancy*
514 *Estimation and Modeling: Inferring Patterns and Dynamics of Species Occurrence.*
515 Academic Press.
516 MacKenzie, D.I., Nichols, J.D., Hines, J.E., Knutson, M.G. & Franklin, A.B. (2003).
517 Estimating site occupancy, colonization, and local extinction when a species is detected
518 imperfectly. *Ecology*, 84, 2200–2207.
519 MacKenzie, D.I., Nichols, J.D., Lachman, G.B., Droege, S., Andrew Royle, J. & Langtimm,
520 C.A. (2002). Estimating site occupancy rates when detection probabilities are less than
521 one. *Ecology*, 83, 2248–2255.
522 McClenaghan, B., Compson, Z. & Hajibabaei, M. (2020). Validating metabarcoding-based
523 biodiversity assessments with multi-species occupancy models: A case study using
524 coastal marine eDNA. *PLoS One*, 15, e0224119.
525 Pacifici, K., Reich, B.J., Dorazio, R.M. & Conroy, M.J. (2016). Occupancy estimation for
526 rare species using a spatially-adaptive sampling design. *Methods Ecol. Evol.*, 7, 285–
527 293.
528 Pillans, B. (2017). Quaternary stratigraphy of Whanganui Basin—a globally significant
529 archive. In: *Landscape and Quaternary Environmental Change in New Zealand* (ed.
530 Shulmeister, J.). Atlantis Press, Paris, pp. 141–170.

Proust, J.N., Lamarche, G., Nodder, S. & Kamp, P.J. (2005). Sedimentary architecture of a Plio-Pleistocene proto-back-arc basin: Wanganui Basin, New Zealand. *Sediment. Geol.*, 181, 107–145.

Royle, J.A. (2004). N-Mixture models for eestimating population size from spatially replicated counts. *Biometrics*, 60, 108–115.

Royle, J.A., Nichols, J.D. & Kéry, M. (2005). Modelling occurrence and abundance of species when detection is imperfect. *Oikos*, 110, 353–359.

Schmettow, M. (2009). Controlling the usability evaluation process under varying defect visibility. In: *Proceedings of the 2009 British Computer Society Conference on Human-Computer Interaction*. pp. 188–197.

Da Silva Neto, J.G., Sutton, W.B., Spear, S.F., Freake, M.J., Kéry, M. & Schmidt, B.R. (2020). Integrating species distribution and occupancy modeling to study hellbender (Cryptobranchus alleganiensis) occurrence based on eDNA surveys. *Biol. Conserv.*, 251, 108787.

Sosdian, S. & Rosenthal, Y. (2009). Deep-sea semperature and ice volume changes ccross the Pliocene-Pleistocene climate transitions. *Science (80-.).*, 325, 306 LP – 310.

Sutherland, W.J., Freckleton, R.P., Godfray, H.C.J., Beissinger, S.R., Benton, T., Cameron, D.D., *et al.* (2013). Identification of 100 fundamental ecological questions. *J. Ecol.*, 101, 58–67.

Yamaura, Y., Andrew Royle, J., Kuboi, K., Tada, T., Ikeno, S. & Makino, S. (2010). Modelling community dynamics based on species-level abundance models from detection/nondetection data. *J. Appl. Ecol.*, 48, 67–75.

554 **Figure captions**

555 **Figure 1:** Each thick bordered open rectangle represents a time-interval (two are illustrated
556 more fully, the first time-interval, T1, and the n^{th} time-interval, Tn). Within each time-
557 interval, Sites (dotted rectangles) are sampled (two are more fully illustrated in each). Within
558 each site, there are subsamples (smaller, solid bordered rectangles) in which different species
559 (solid shapes) are observed. The open circle represents the super species, which in our case,
560 we assume to be present in all sites, even if not sampled in all subsamples.
561

562 **Figure 2.** This figure summarizes our full hierarchical occupancy model, TRAMPOline,
563 composed of top parameters and random factors that describe their overdispersion (Eqn 5).
564 Data are denoted as triangles where N are the number of sites and y the shells from site i
565 where species s is observed. Black circles denote occupancy parameters, white circles denote
566 detection parameters and grey circle denotes the overdispersion parameter. An arrow from an
567 element A (i.e. circle, triangle or rectangle) to another B, denotes that B is conditioned on A
568 either by a function or a distribution (see text for details).
569

570 **Figure 3.** Estimates are from our full model where black lines join the species posterior
571 median occupancy for each formation (time-interval) plotted in the middle of the age range of
572 the given formation. Grey lines show 95% posterior credibility intervals for the estimates.
573 Note that the superspecies is not plotted here as its occupancy is assumed to be 1 throughout.
574

575 **Figure 4: Estimated detection probabilities.** Estimates are from our full model where black
576 lines join the species median detection probabilities (plotted on log scale) for each formation
577 (time-interval). Grey lines show 95% posterior credibility intervals for the estimates.

578

579 **Figure 5: Estimated relative abundance.** Estimates are from our full model where black
580 lines join the species mean relative abundance (plotted on a log scale, except for the
581 Superspecies for visibility) for each formation (time-interval). Grey lines show 95% posterior
582 credibility intervals for the estimates.

583

584 **Figure 6: Relative abundances from the parameter-focused simulation study.** Solid lines
585 show the true relative abundances for the various species and formations, while the points are
586 estimates from the 100 simulated datasets.

587 **Figure 1: A schematic diagram to show the sampling scheme for TRAMPOline**

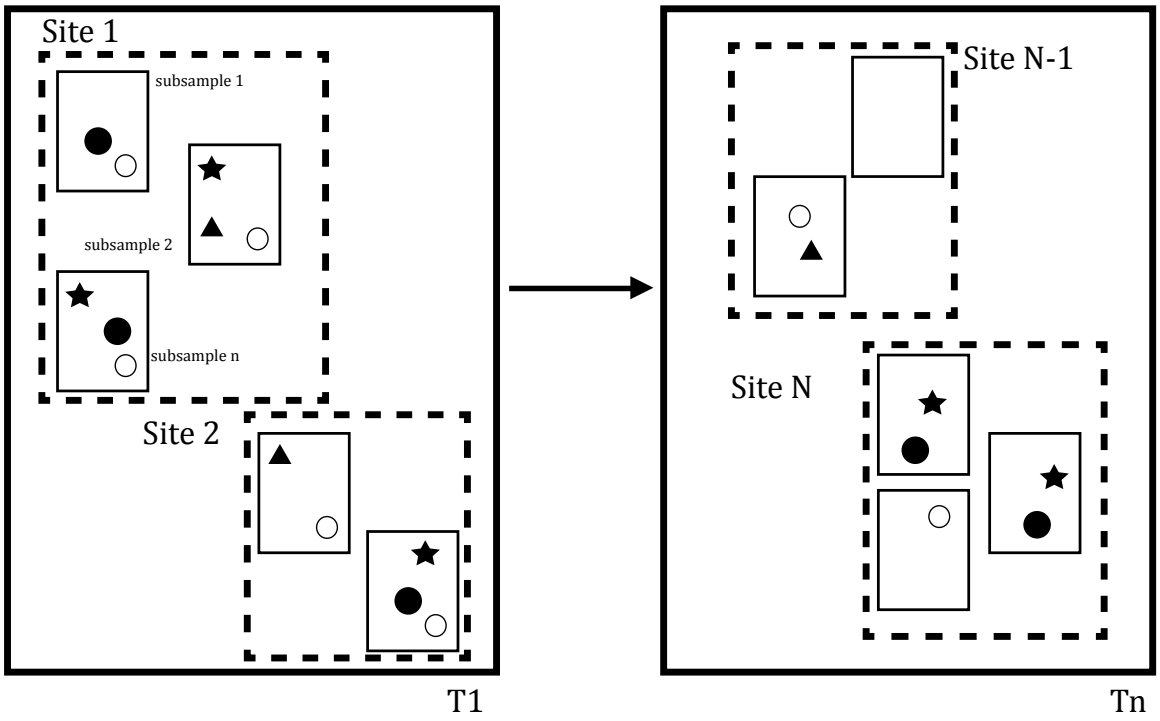

588

589

590

Figure 2: TRAMPOline: Full hierarchical occupancy model to estimate relative abundance

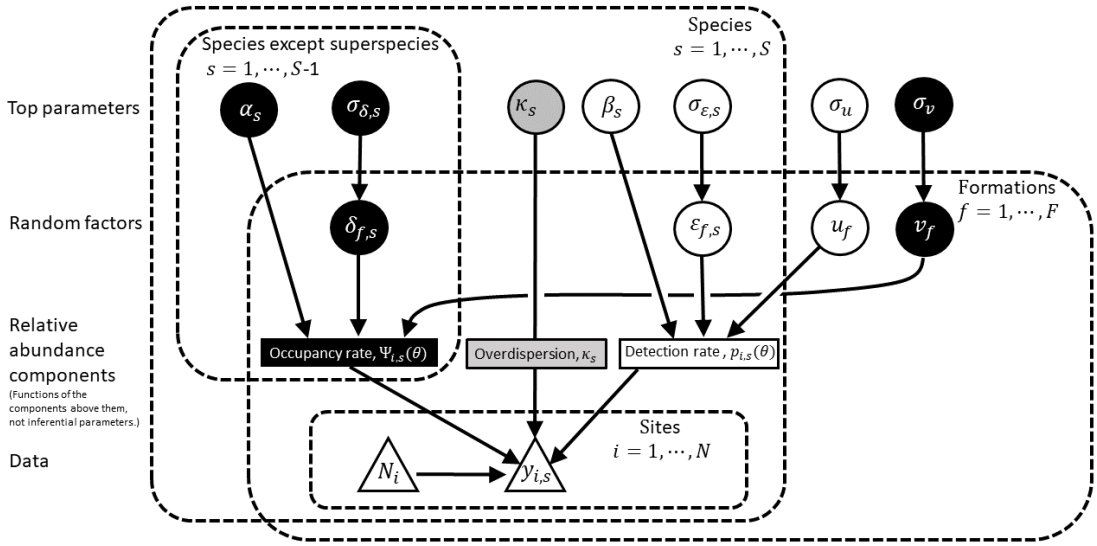

596 **Figure 3: Estimated occupancy probabilities for the three focal species.**

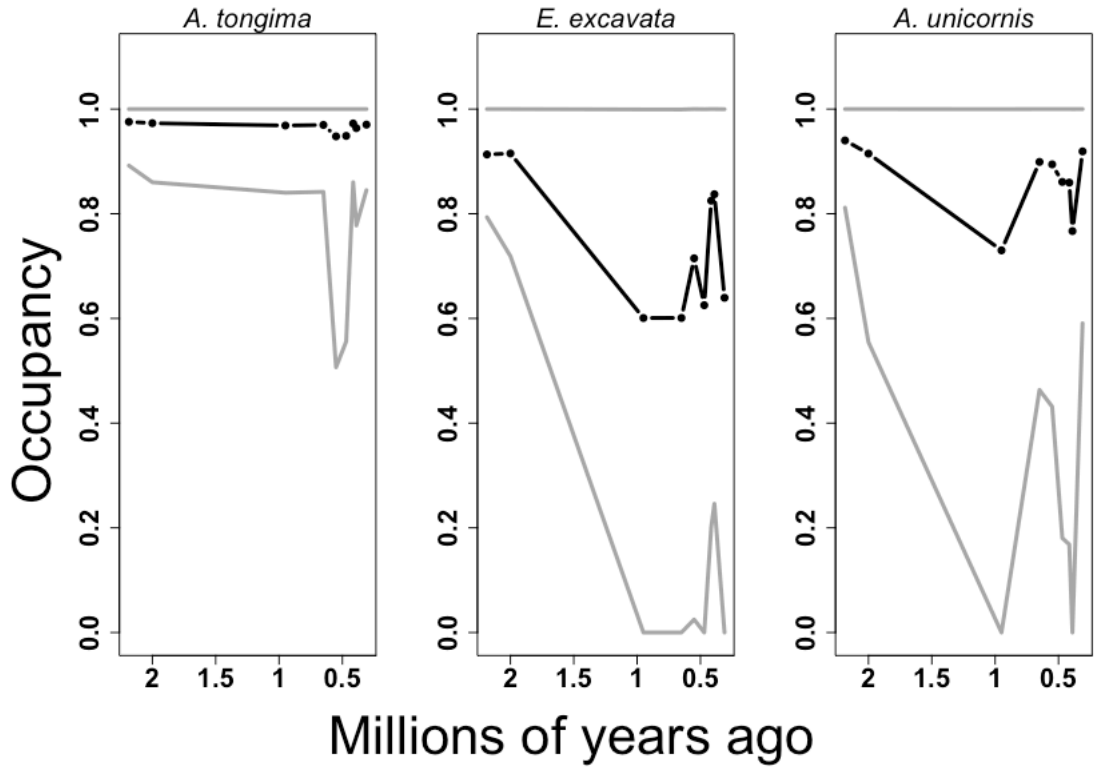

597

598

599 **Figure 4: Estimated detection probabilities.**

600

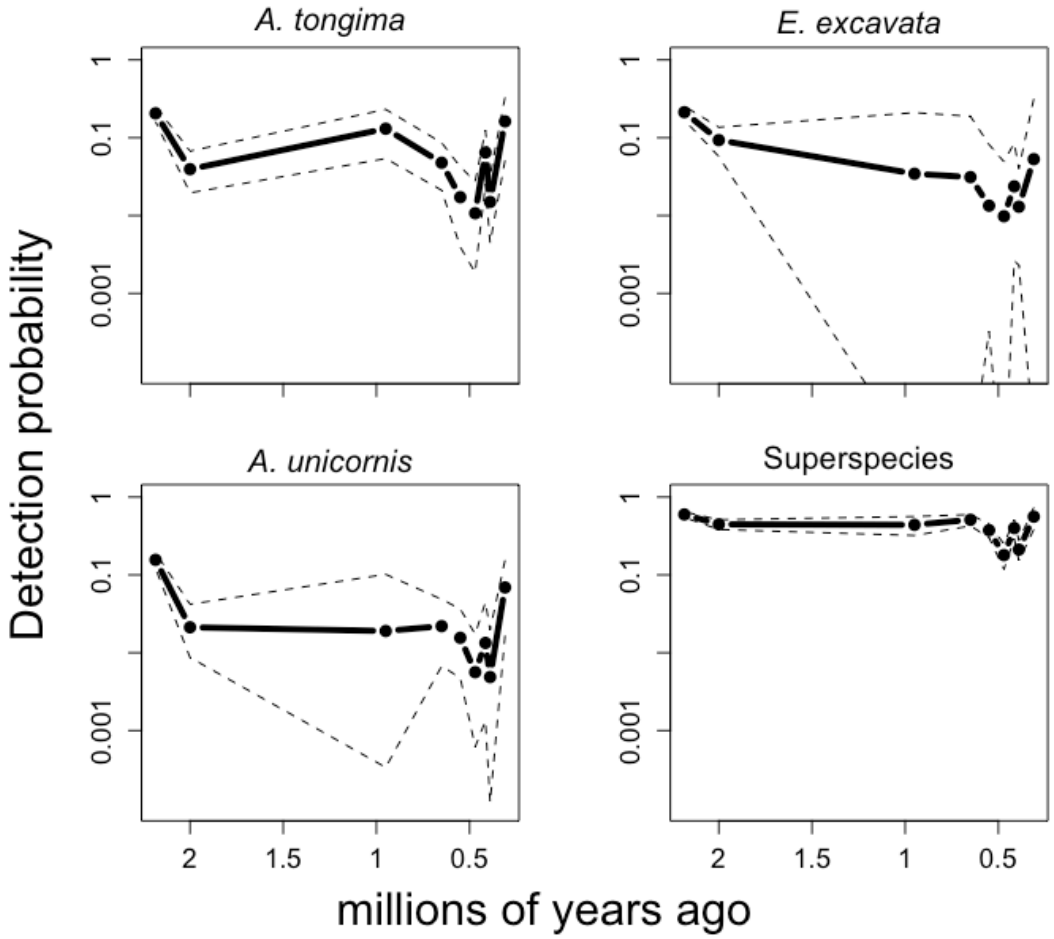

601

602 **Figure 5. Estimated relative abundance.**

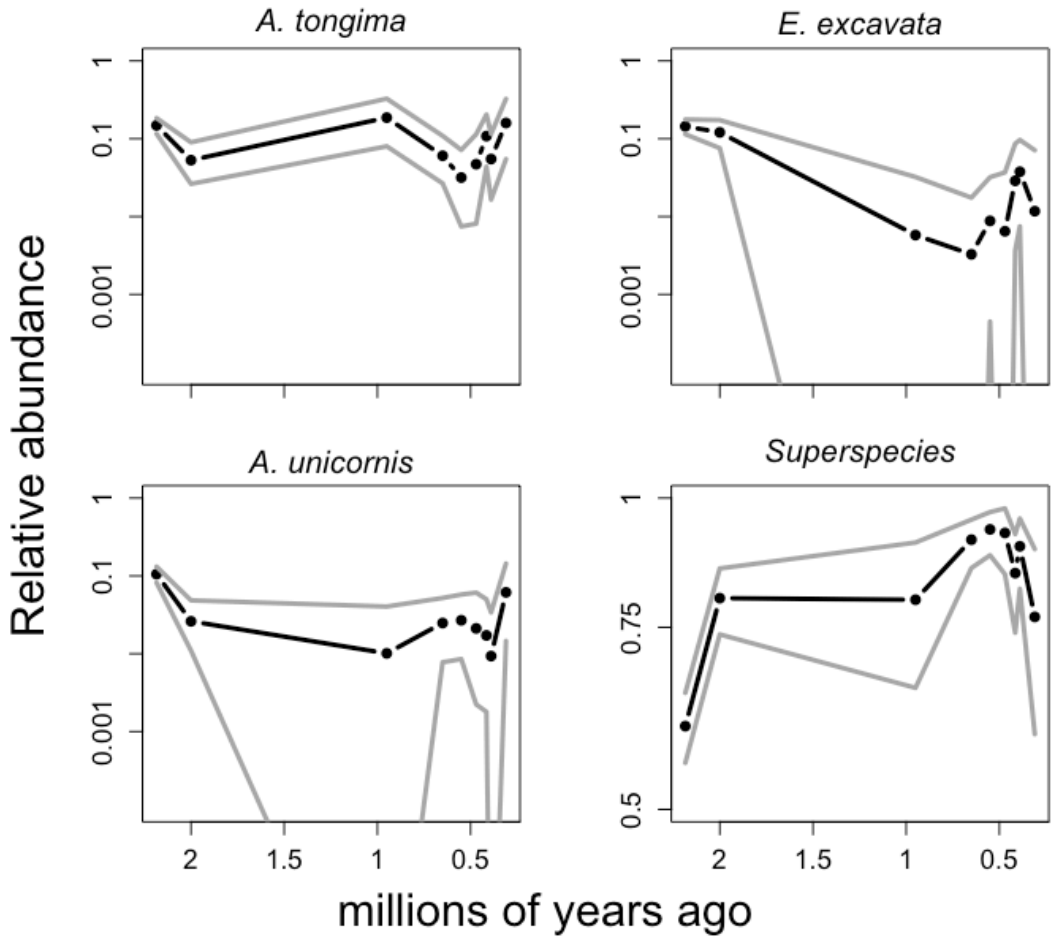

603

604

605 **Figure 6: Relative abundances from the parameter-focused simulation study.**

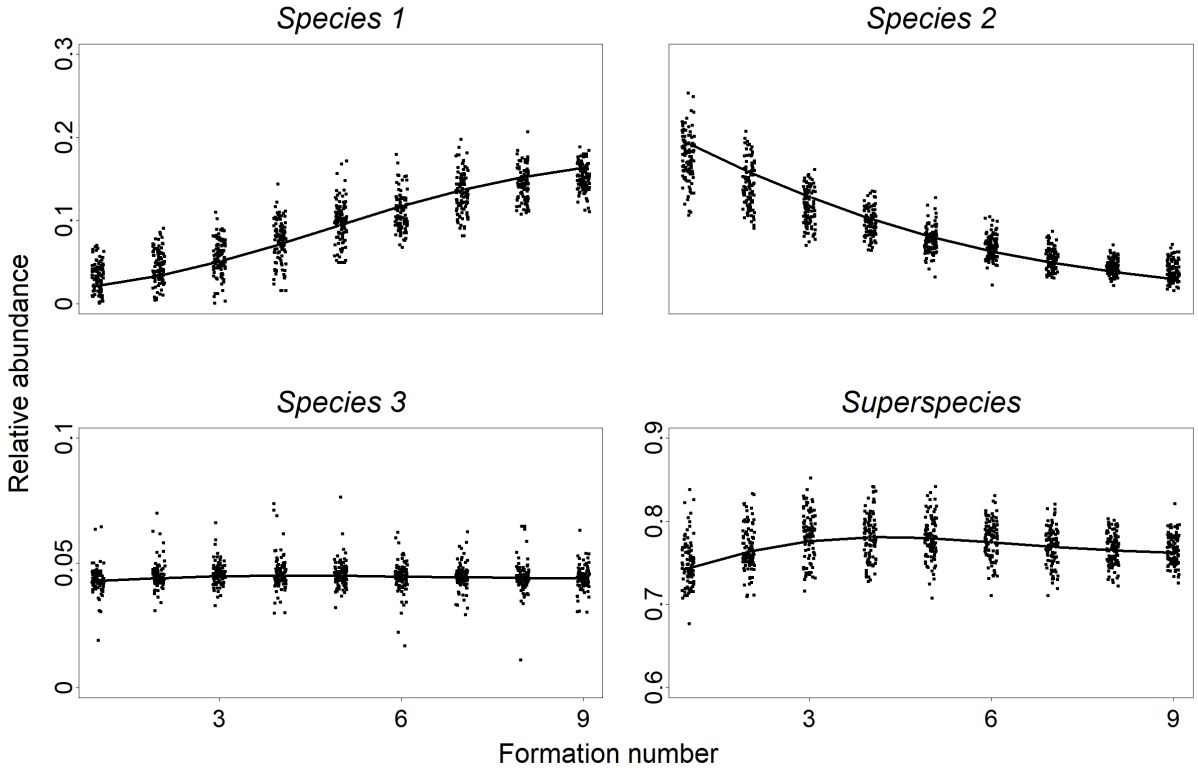

606